environmental microbiology reports

Environmental Microbiology Reports (2021) **00**(00), 00–00 doi:10.1111/1758-2229.13011

Brief Report

Cyanobacterial community composition and their functional shifts associated with biocrust succession in the Gurbantunggut Desert

Shubin Lan,[1*] Andrew David Thomas,[2] Julie Bethany Rakes,[3] Ferran Garcia-Pichel,[3] Li Wu[4] and Chunxiang Hu[1]

[1]*Key Laboratory of Algal Biology, Institute of Hydrobiology, Chinese Academy of Sciences, Wuhan, 430072, China.*

[2]*Department of Geography and Earth Sciences, Aberystwyth University, Aberystwyth, SY23 3DB, UK.*

[3]*School of Life Sciences and Center for Fundamental and Applied Microbiomics, Arizona State University, Tempe, AZ, 85287.*

[4]*School of Resources and Environmental Engineering, Wuhan University of Technology, Wuhan, 430072, China.*

Summary

Cyanobacteria, as key biocrust components, provide a variety of ecosystem functions in drylands. In this study, to identify whether a cyanobacterial community shift is involved in biocrust succession and whether this is linked to altered ecological functions, we investigated cyanobacterial composition, total carbon and nitrogen contents of biocrusts in the Gurbantunggut Desert. Our findings showed that the biocrust cyanobacteria in the Gurbantunggut desert were mostly filamentous, coexisting with abundant unicellular colonial *Chroococcidiopsis*. Heterocystous *Nostoc*, *Scytonema* and *Tolypothrix* always represented the majority of biocrust nitrogen-fixing organisms, comprising an average of 92% of the nifH gene reads. Community analysis showed a clear shift in prokaryotic community composition associated with biocrust succession from cyanobacteria- to lichen- and moss-dominated biocrusts, and filamentous non-nitrogen-fixing cyanobacteria-dominated communities were gradually replaced by nitrogen-fixing and unicellular colonial communities. Along the succession, there were concomitant reductions in cyanobacterial relative abundance, whereas Chl-a, total carbon and nitrogen contents increased. Concurrently, distinct carbon and nitrogen stores shifts occurred, implying that the main ecological contribution of cyanobacteria in biocrusts changes from carbon- to nitrogen-fixation along with the succession. Our results suggest that any activity that reverses biocrust succession will influence cyanobacterial community composition and eventually lead to large reductions in soil carbon and nitrogen stores.

Introduction

Drylands account for more than 40% of the global land area (Reynolds *et al*., 2007; Roncero-Ramos *et al*., 2019), where vascular plants are often sparsely distributed due to limited water and soil resources. However, the gaps between vascular plants are commonly covered with biological soil crusts or biocrusts, forming a mosaic of macroscopic vascular plants and microscopic biocrust patches across the landscapes (Elliott *et al*., 2014; Lan *et al*., 2019). Biocrusts, as a layer of topsoil assemblages composed of photoautotrophic and heterotrophic microorganisms, provide a variety of ecosystem services and functions in drylands, such as protecting soil from erosion (Eldridge and Leys, 2003; Rodríguez-Caballero*et al*., 2012), influencing hydrologic soil properties (Belnap, 2006; Felde *et al*., 2014) and enhancing soil fertility through photosynthesis and nitrogen fixation (Elbert *et al*., 2012; Thomas, 2012; Büdel *et al*., 2014; Rodriguez-Caballero *et al*., 2018; Thomas *et al*., 2018).

Cyanobacteria, especially filamentous cyanobacteria, such as *Microcoleus*, are often the main photosynthetic colonists involved with the initial establishment of biocrusts due to their unique physiological and ecological characteristics (Garcia-Pichel and Pringault, 2001; Wu *et al*., 2013; Lan *et al*., 2014). Therefore, cyanobacterial soil crusts (cyanobacteria-dominated biocrusts with very limited lichens and mosses; Wu *et al*., 2014) are

Received 6 May, 2021; accepted 4 September, 2021. *For correspondence. E-mail shblan@ihb.ac.cn. Tel/Fax: 0086-27-68780046.

generally regarded as the primary or early successional stages, which gradually improve the soil surface microenvironments and provide the opportunities for colonization of later successional lichens and/or mosses (Zaady *et al*., 2000; Belnap, 2006). The photosynthetic dominants change through time during this process, resulting in biocrusts characterized by varying proportions of cyanobacteria, lichens and mosses (Housman *et al*., 2006; Zhang *et al*., 2007 Maier *et al*., 2018). Changes to the dominant species and community composition both stimulate and underpin biocrust ecological succession (Hagemann *et al*., 2014; Lan *et al*., 2014). In turn, different dominant photoautotrophic types associated with biocrust succession control microbial diversity, pigment composition and physiology (Lan *et al*., 2017; Maier *et al*., 2018).

Biocrust composition is sensitive to climate change and land disturbance, with a recent estimate suggesting that the global distribution of biocrusts could decrease by 25%–40% in the next 65 years (Rodriguez-Caballero *et al*., 2018). However, the extent to which biocrust are affected by climatic and land disturbance is still largely dependent upon their species composition. Eldridge and Delgado-Baquerizo (2019) reported that the decrease of relative abundance in biocrust *Peltulaceae*, *Teloschistaceae* and *Bryaceae* was related to the positive temperature legacies (temperature increased), while increase in relative abundances of *Cladoniaceae*, *Lecideaceae*, *Thelotremataceae* and *Pottiaceae* was related to the positive precipitation legacy (precipitation increased). Furthermore, a continental-scale biocrust survey found cyanobacterium *Microcoleus steenstrupii* to be more thermotolerant but less psychrotolerant than *M. vaginatus* (Garcia-Pichel *et al*., 2013), with recent evidence from Fernandes *et al*. (2018) suggesting that *Scytonema* may be particularly sensitive to decreased precipitation, followed by *M. steenstrupii* and *M. vaginatus*. There is a growing evidence base and consensus that biocrust communities will be affected by future environmental changes, and these changes may convert large areas of later successional biocrusts to early successional stages (Housman *et al*., 2006). However, there is only limited understanding of how cyanobacteria, as the pioneer, important carbon and nitrogen fixers in biocrusts, are linked to biocrust ecological succession. The current simplified model (Garcia-Pichel, 2003) derived from observation in North America suggests that bundle forming non-heterocystous cyanobacteria (*M. vaginatus*, members of the *M. steentrupii* complex) are the pioneers that stabilize the soil (Garcia-Pichel and Wojciechowski, 2009). Once the soil is stable, sessile heterocystous cyanobacteria can colonize (Couradeau *et al*., 2016). The two types occupy differentiated vertical micro-niches (Garcia-Pichel and Belnap, 2001).

We hypothesized that cyanobacterial community shift involved in biocrust ecological succession occurs at finer taxonomic resolution, and that the changes might affect the ecological functions of biocrusts. It is important to obtain a more detailed knowledge in the face of the known differential effects of climate change and soil disturbance on community composition and function. In this study, we investigated cyanobacterial community compositions, and associated ecological parameters (e.g. total carbon and nitrogen stores) in different successional types of biocrusts from the arid Gurbantunggut Desert, China (average annual precipitation 79.5 mm with potential evaporation more than 2600 mm; Zhang *et al*., 2007), to test the validity of current models of cyanobacterial community shift, increase our organismal resolution involved in biocrust succession, and lastly to assess if cyanobacterial community shift correlates with biocrust carbon and nitrogen stores.

Results

Cyanobacterial diversity and community structure

A total of 460 987 valid sequences (1121 OTUs) were obtained from four successional types of biocrusts (with four replicates of each giving a total of 16 samples) using 16S rRNA gene high-throughput sequencing (Table 1). The majority (87.82%) of sequences were assigned to 16 Phyla, and the remaining sequences were annotated as candidate divisions BJ-169, BRC1, FBP and unclassified (others in Fig. 1). The most abundant phyla were Cyanobacteria (26.05% of the total reads across all samples), Actinobacteria (23.29%) and Proteobacteria (21.16%); followed by Chloroflexi (5.20%), Acidobacteria (3.41%), Bacteroidetes (3.27%), Planctomycetes (2.13%) and Gemmatimonadetes (1.45%; Fig. 1A), although this varied depending on the successional types of biocrusts (Fig. 1B).

Table 2 shows the taxonomic assignments of cyanobacterial operational taxonomic units (OTUs) based on their positions within the phylogenetic trees constructed using 16S rRNA gene sequences (Fig. 2A and B). A total of 47 cyanobacterial OTUs were identified through the 16S rRNA gene sequences, which were divided into 20 Clades (Fig. 2; Table 2). Only two Clades including 10 OTUs were identified as unicellular colonial cyanobacteria belonging to genus *Chroococcidiopsis*; while 13 Clades (28 OTUs) were identified as non-nitrogen-fixing filamentous cyanobacteria, including *Crinalium*, *Lyngbya*, *Microcoleus*, *Oculatella*, *Pseudophormidium* and *Trichocoleus* (Fig. 2A and B). The most abundant Clade 13 was assignable to *M. vaginatus*, which accounted for 43% of the total cyanobacterial sequences, followed by Clade16 (*Nostoc* spp.; 12.67%), Clade8

Table 1. Biocrust development status and basic characteristics derived from high-throughput sequencing.

Sample code	ESCs	DSCs	LSCs	MSCs
Successional type	Early cyanobacterial soil crusts	Developed-cyanobacterial soil crusts	Lichen soil crusts	Moss soil crusts
Colour	Light grey	Dark grey	Black	Brown
Dominants	*Microcoleus* spp.	*Microcoleus* spp.	*Collema*	*Bryum*
Thickness (mm)	1.82–3.95	2.29–3.92	6.42–8.32	11.80–12.94
Development index	0.03–0.10	0.05–0.18	0.14–0.32	0.87–0.97
16S rRNA gene reads	26 538–28 315	23 912–30 216	28 280–31 782	24 636–32 432
Cyanobacterial reads (16S rRNA)	7289–10 837	4591–11 752	7736–12 137	1892–5019
Cyanobacterial OTUs (16S rRNA)	38	46	46	45
nifH gene reads	27 054–54 404	33 383–44 808	27 732–44 172	28 873–31 672
Cyanobacterial reads (nifH)	20 494–47 993	27 652–43 779	27 151–43 735	26 556–30 464
Cyanobacterial OTUs (nifH)	30	30	31	31

(*Chroococcidiopsis* spp.; 12.43%), Clade15 (*M. steenstrupii*; 11.28%) and Clade18 (*Scytonema hyalinum* 275; 5.17%). The remaining 15 Clades accounted for a total of 15.45% of cyanobacterial sequences (Fig. 3A).

The nine nitrogen-fixing cyanobacterial OTUs together accounted for 23.48% of the total 16S rRNA gene reads (Figs 3A and 4B). The phylotypes corresponding to *Nostoc* (OTUs96, 482 and 555) and *Tolypothrix* (OUT310) fell into their respective Clades gathering representative sequences from each genus; while *Scytonema* phylotypes (OUTs 78, 275, 298, 406 and 861) were mapped into three different Clades (Fig. 2B). Both OTU275 and OTU861 were identified as *S. hyalinum*, although they belonged to two Clades respectively. In addition, based on the nifH gene sequences, 31 nitrogen-fixing cyanobacterial OTUs were mapped into five Clades (Fig. 2C). However, according to the nifH gene, phylotypes of *Scytonema* (10 OTUs) detected in our study fell into a separated Clade, while *Nostoc* phylotypes (19 OUTs) were mapped into three different Clades (Fig. 2C).

Cyanobacterial community shift associated with biocrust succession

16S rRNA gene results showed cyanobacterial relative abundance gradually decreased along with the increasing developing index from early cyanobacterial (ESCs), developed-cyanobacterial (DSCs), to lichen (LSCs) and moss soil crusts (MSCs; $P < 0.05$; Table 1; Fig. 4A), but the relative abundance of nitrogen-fixing cyanobacteria in the whole cyanobacterial community increased with very dominant forms (i.e., *Microcoleus vaginatus*) losing ground to other forms ($P < 0.05$; Fig. 4B). The heterocystous nitrogen-fixing cyanobacteria accounted for 92.78% of the nitrogen-fixing microorganisms dwelling in the biocrusts (indicated by the nifH gene), and there was no significant difference between the different successional types ($P > 0.05$; Fig. 4A). Furthermore, the relative abundance of unicellular colonial cyanobacteria (*Chroococcidiopsis*) in the whole cyanobacterial community increased ($P < 0.05$), while the relative abundance of the filamentous non-nitrogen-fixing cyanobacteria decreased gradually along with biocrust succession ($P < 0.05$; Fig. 4B).

Except for Clades 2, 10 and 19, relative abundance for all the other cyanobacterial Clades was significantly different depending on biocrust successional types ($P < 0.05$; Table 2). Cyanobacterial community analysis revealed that the relative abundance of *M. vaginatus* decreased along with the succession, while members of the *M. steenstrupii complex* showed a significant increasing trend (Fig. 3A; Table 2). Similarly, with the succession of biocrusts, *Chroococcidiopsis* spp., *Oculatella* spp., *Nostoc* spp., *S. hyalinum* 861, *S. hyalinum* 275 and *Tolypothrix distorta* showed an increasing trend (Fig. 3A). Considering ESCs and DSCs as a whole (as well as lichen and moss soil crusts as a whole; LSCs and MSCs), a significantly increased relative abundance was observed for the Clades assigned as *Chroococcidiopsis* spp., *Microcoleus* sp. 1, *Microcoleus* spp., *Nostoc* spp., *Oculatella* spp., *Pseudophormidium* sp., *S. hyalinum* 275, *S. hyalinum* 861, *Scytonema* spp. and *T. distorta* in LSCs and MSCs compared with early cyanobacterial ESCs and DSCs; while the decrease was obtained for *Crinalium* sp. 1, *Crinalium* sp. 2, *Crinalium* sp. 3, *Lyngbya* sp., *M.* cf. *chthonoplastes*, *Microcoleus sociatus* and *M. vaginatus* (Fig. S2A and B).

At genus level, the relative abundance for every genus was significantly different among the different successional types ($P < 0.05$; Table S1). Overall, *Microcoleus*, *Chroococcidiopsis*, *Nostoc* and *Scytonema* are the main genera found in the biocrusts from the Gurbantunggut Desert, accounting for 92.70% of the entire cyanobacterial community. Compared with ESCs and DSCs, LSCs and MSCs had a higher relative abundance in the genera *Chroococcidiopsis*, *Nostoc*, *Oculatella*, *Pseudophormidium*, *Scytonema* and *Tolypothrix*; while early cyanobacterial and developed-cyanobacterial soil crusts (ESCs and DSCs) had a higher relative

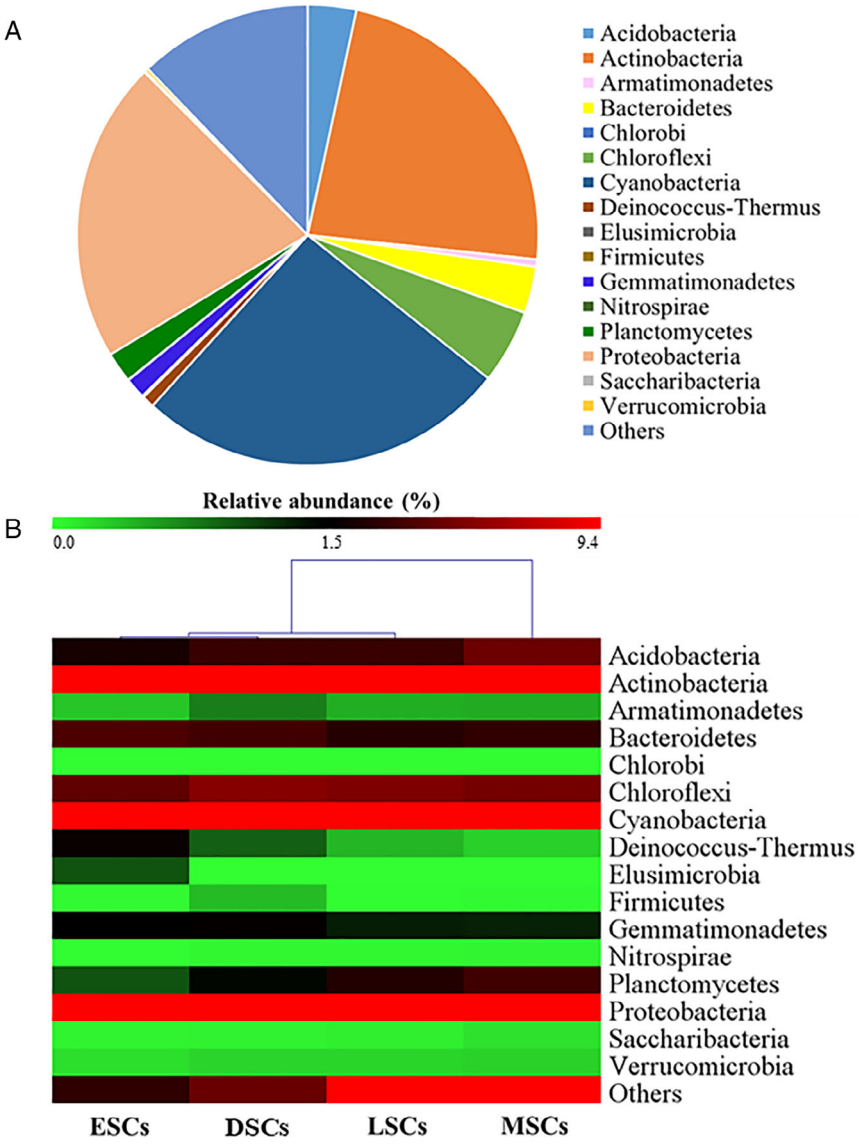

Fig. 1. Biocrust bacterial community structure at phylum level based on 16S rRNA gene sequences.A. Relative abundance of bacterial compositions at phylum level averaged over all biocrust samples.B. Clustering heatmap of bacterial community structures at phylum level (see Table 1 for the definition of abbreviations of biocrust sample code).

abundance of sequences in the genera *Crinalium*, *Lyngbya* and *Microcoleus* (Fig. S2C and D).

Total carbon, total nitrogen and pigment content

From ESCs, DSCs, to LSCs and MSCs, biocrust chlorophyll-a (Chl-a) and carotenoid contents gradually increased, although the difference between any two successional types was not always significant at 0.05 level (Fig. 5A and B). Scytonemin content was highest in the LSCs, and all pigment contents were lowest in the ESCs (Fig. 5). In particular, the scytonemin content in ESCs was only 3.74% of that in the LSCs. In addition, there was a linear positive correlation between Chl-a and carotenoid content ($R^2 = 0.826$; $P < 0.001$), and the ratio of carotenoid to Chl-a content was maintained at 0.18 (Fig. S3A). By contrast, biocrust scytonemin content increased and then decreased with the increasing Chl-a content ($R^2 = 0.544$; $P = 0.002$; Fig. S3A).

Total carbon and total nitrogen contents of the biocrusts ranged from 4.22 to 23.50 g kg^{-1} and 0.51 to 1.49 g kg^{-1} respectively, and there were significant differences between biocrust types ($P < 0.05$; Fig. 4C). Both total carbon and total nitrogen contents gradually increased with biocrust succession (from ESCs to MSCs), and the ratio of total carbon to total nitrogen was consistent at around 13.5, ($R^2 = 0.604$; $P < 0.001$, Fig. S3B).

Table 2. Taxonomic assignments of operational taxonomic units (OTUs) based on 16S rRNA gene sequences and the non-parametric test of their relative abundance variation depending on biocrust successional types.

Clade number	Taxa	OTUs	Species from NCBI (accession no.)	X^2	df	P
Clade 1	*Pseudophormidium* sp.[a]	OTU347	*Pseudophormidium* sp. WJT61-NPBG13 (KJ939055)	11.805	3	0.008
Clade 2	*Chroococcidiopsis* sp.	OTU891	*Chroococcidiopsis* sp. MKC.28 (MF467540)	4.848	3	0.183
Clade 3	*Crinalium* sp. 1	OTU11	*Crinalium epipsammum* SAG 22.89 (NR 112218)	8.365	3	0.039
Clade 4	*Trichocoleus desertorum*[a]	OTU276	*Trichocoleus desertorum* 64et (KX759133); *Trichocoleus desertorum* Mon69 D (MK478718)	8.568	3	0.036
Clade 5	*Crinalium* sp. 2	OTU172	*Crinalium* sp. UMPCCC 1112 (KM218881)	13.792	3	0.003
Clade 6	Crinalium sp. 3	OTU445	*Crinalium* sp. UMPCCC 1112 (KM218881)	9.253	3	0.026
Clade 7	*Lyngbya* sp.	OTU20	*Lyngbya aestuarii* ISB52 (KY349108)	12.295	3	0.006
Clade 8	*Chroococcidiopsis* spp.	OTU305; OTU493; OTU530; OTU483; OTU583; OTU264; OTU485; OTU1053	*Chroococcidiopsis thermalis* CHAB1690 (JX494785); *Chroococcidiopsis* sp. BB79.2 SAG 2023 (AJ344552); *Chroococcidiopsis* sp. CCMEE 246 (JF810073); *Chroococcidiopsis* sp. A789-2 (JF810071); *Chroococcidiopsis* sp. CC1 (DQ914863.2); *Chroococcidiopsis* sp. UFS-A4UI-NPMV4-B4 (KC525099); *Chroococcidiopsis* sp. CXA029 4 (MH463398)	10.522	3	0.015
Clade 9	*Oculatella* spp.	OTU394; OTU494; OTu1075	*Oculatella* sp. ATA1-4-EC o7 (KF761568)	9.142	3	0.027
Clade 10	*Microcoleus sociatus*	OTU75; OTU512	*M. sociatus* SAG 26.92 (AF284808); *M. sociatus* MPI 96MS.KID (AF284809)	5.051	3	0.168
Clade 11	*Microcoleus* cf. *chthonoplastes*	OTU21	*Microcoleus* cf. *chthonoplastes* Es Yyy1100 (KC463182)	11.471	3	0.009
Clade 12	*Microcoleus* spp.	OTU284; OTU348		9.375	3	0.025
Clade 13	*Microcoleus vaginatus*	OTU74; OTU571	*M. vaginatus* KZ-23-1 (MK211228); *M. vaginatus* USPCI-1 (EU586737); *M. vaginatus* 127–1 (AJ871222); *M. vaginatus* Pasv-RS27 (KU175689)	11.669	3	0.009
Clade 14	*Microcoleus* sp.	OTU505		10.318	3	0.016
Clade 15	*M. steenstrupii*	OTU306; OTU475; OTU480; OTU486; OTU487; OTU286; OTU19; OTU77; OTU481; OTU283; OTU612	*M. steenstrupii* 177-4B (AF355392); *M. steenstrupii* 177-7A (AF355395); *M. steenstrupii* ATA12-3-DP02 (KC311865); *M. steenstrupii* 187–2 (AJ871986); *M. steenstrupii* COL109 (KC999638); *M. steenstrupii* 141–2 (AJ871981); *M. steenstrupii* 129–1 (AJ871979)	9.86	3	0.02
Clade 16	*Nostoc* spp.	OTU96; OTU482; OTU555	*Nostoc* cf. *indistinguendum* F15-VF4 (AY577540); *Nostoc* sp. Lukesova 5/96 (AM711546); *Nostoc punctiforme* KZ-2-2-2 (MK211227); *Nostoc commune* Mon62 A (MK478701); *Nostoc flagelliforme* str. Sunitezuoqi (GU810186)	8.647	3	0.034
Clade 17	*Tolypothrix distorta*	OTU310	*Tolypothrix* sp. Ep Yyy1400 (KC463234); *T. distorta* CAU13 (MG641916)	9.088	3	0.028
Clade 18	*S. hyalinum* 275	OTU275	*S. hyalinum* Mon66 C (MK478708)	12.463	3	0.006
Clade 19	*Scytonema* spp.	OTU78; OTU298; OTU406	*Scytonema* sp. CMT-2BRIN-HLNPC8 CGSFD17 (KF934149)	7.699	3	0.053
Clade 20	*S. hyalinum* 861	OTU861	*S. hyalinum* rrn 1 (MF574180); *S. hyalinum* AM54C (MG641906)	11.206	3	0.011

[a]Clades 1 and 4 include the species in genus *Leptolyngbya*, thus the OTU347 and OTU276 may also be *Leptolyngbya* spp. In this table, we just classified the two OTUs based on the minimum genetic distances with *Pseudophormidium* sp. WJT61-NPBG13 (KJ939055) and *Trichocoleus desertorum* 64et (KX759133).

Fig. 2. Phylogenetic trees of biocrust cyanobacterial OTUs.A. Maximum-likelihood tree of the biocrust cyanobacterial OTUs based on 16S rRNA gene sequences.B. Maximum-likelihood tree of the biocrust nitrogen-fixing cyanobacterial OTUs based on 16S rRNA gene sequences. C. Maximum-likelihood tree of the biocrust nitrogen-fixing cyanobacterial OTUs based on nifH gene sequences. OTU-x indicates the biocrust cyanobacterial OTUs in our study, and the text in brackets shows the GenBank (NCBI) accession numbers of the retrieved cyanobacterial sequences.

Discussion

In this study, we investigated cyanobacterial communities of biocrusts in the extreme arid Gurbantunggut desert. The cyanobacterial community in this region may represent the changing trend of many biocrust cyanobacterial communities from drylands, where aridity has been predicted to increase (Lin *et al*., 2015). Furthermore, we reveal a clear cyanobacterial community shift associated with biocrust succession, and an allied shift in biocrust carbon and nitrogen content.

Cyanobacterial composition and diversity of biocrusts

Studying the composition and diversity of cyanobacteria in biocrusts is an important step towards understanding their ecological functions in drylands. In total,

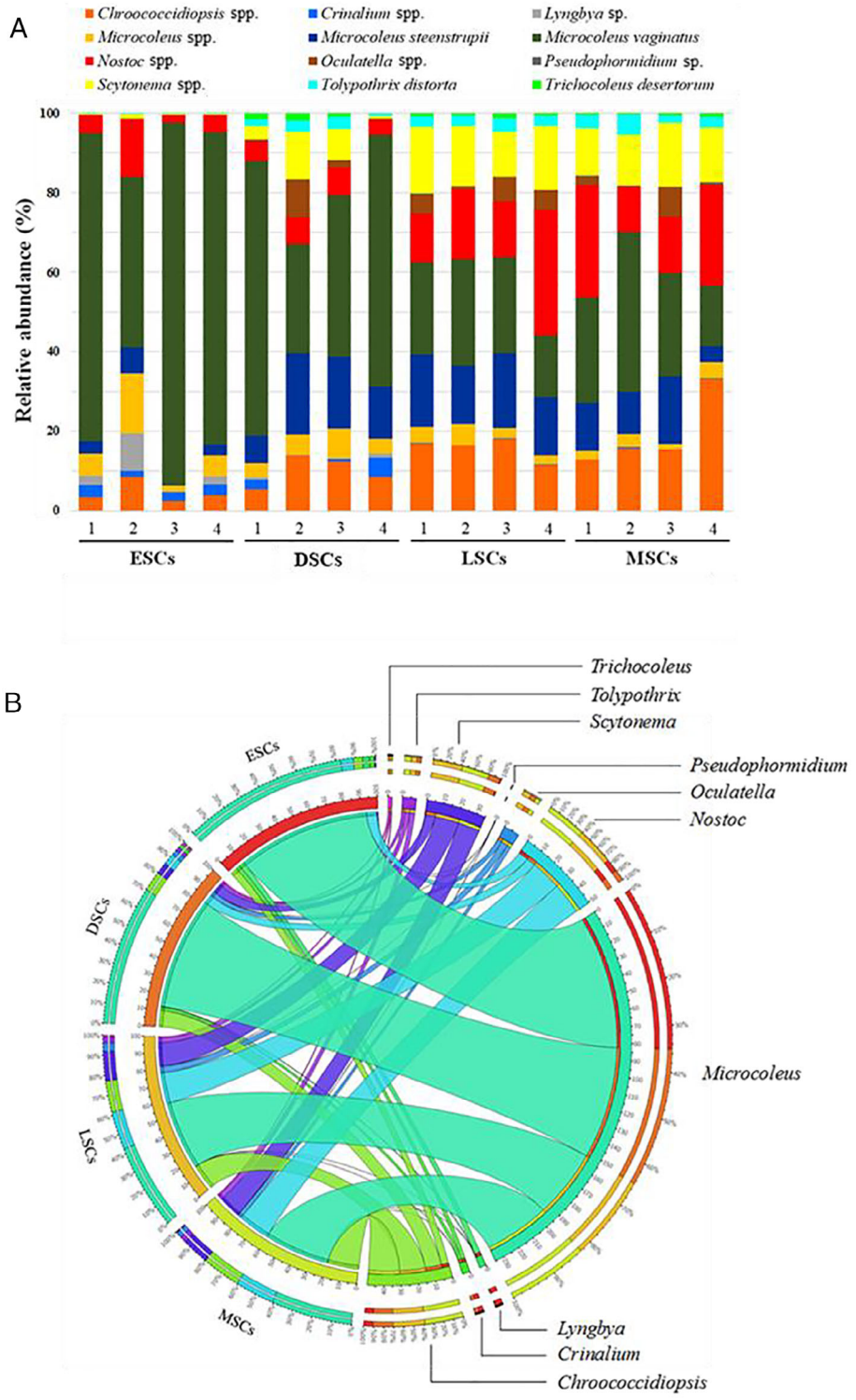

Fig. 3. Cyanobacterial community compositions based on 16S rRNA gene sequences in the different successional types of biocrusts.A. Shifts of different Clades of cyanobacterial phylotypes along with biocrust succession.B. Circos plot showing the average relative abundance of cyanobacterial genera in the different successional types of biocrusts.

47 cyanobacterial OTUs were identified based on 16S rRNA gene sequences; a similar number to that previously reported by Dojani *et al*. (2014) in the succulent Karoo and Nama Karoo of Southern Africa by Steven *et al*. (2012) in the Nevada Desert of North America and by Muñoz-Martín *et al*. (2019) in the eastern Iberian

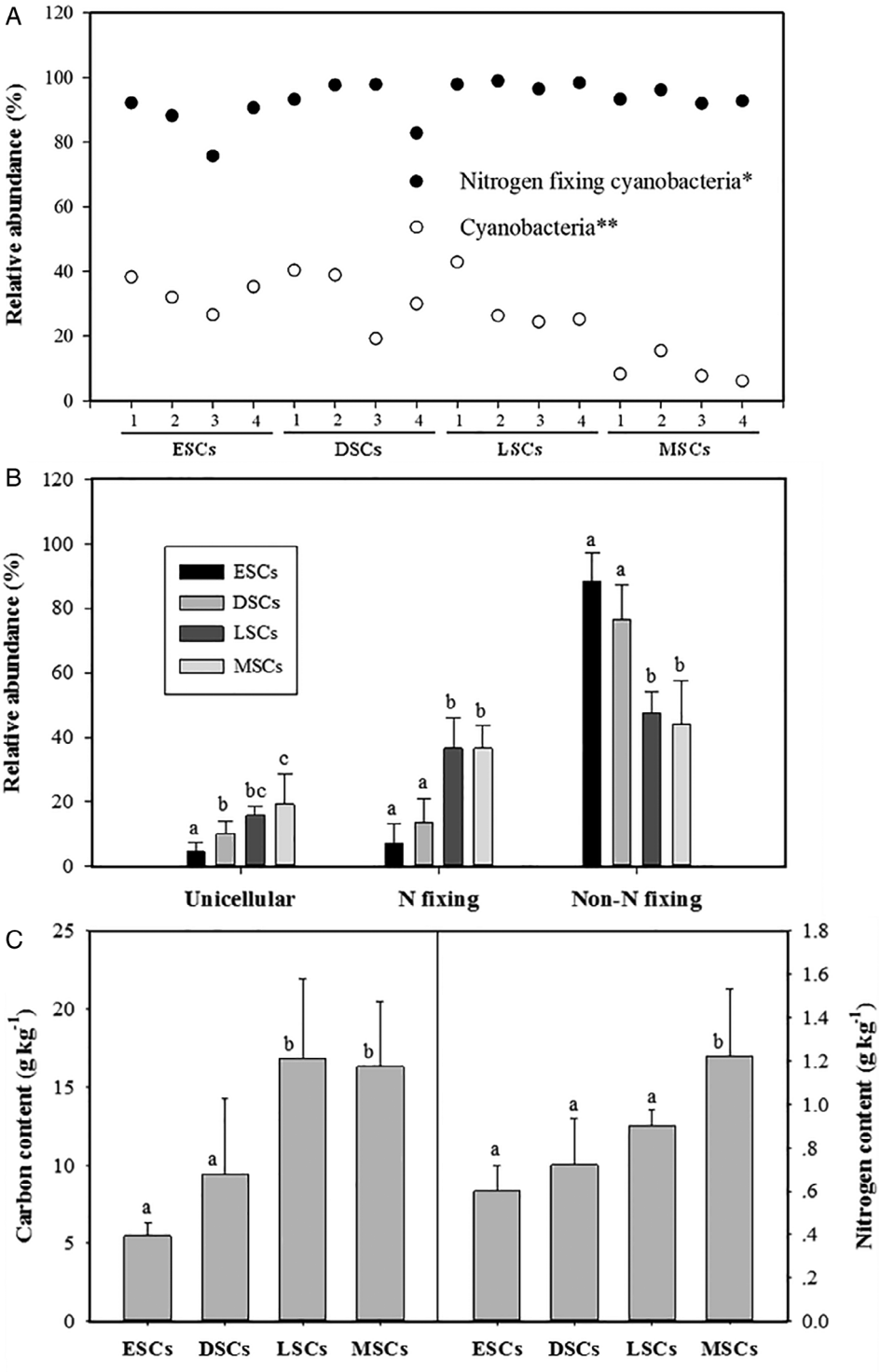

Fig. 4. Cyanobacterial relative abundance, total carbon and total nitrogen content in the different successional types of biocrusts.A. Relative abundance changes of cyanobacterial 16S rRNA genes and nitrogen-fixing cyanobacterial nifH genes along with biocrust succession.B. Relative abundances of the different morphological groups of cyanobacteria (16S rRNA) in the different successional types of biocrusts.C. Total carbon and total nitrogen content in the different successional types of biocrusts. Single asterisk means the relative abundance of nitrogen-fixing cyanobacteria in the whole nitrogen-fixing communities; double asterisk means the cyanobacterial relative abundance in bacterial communities. For each parameter, the different lowercase letters indicate that the values are significantly different at the 0.05 level ($P < 0.05$).

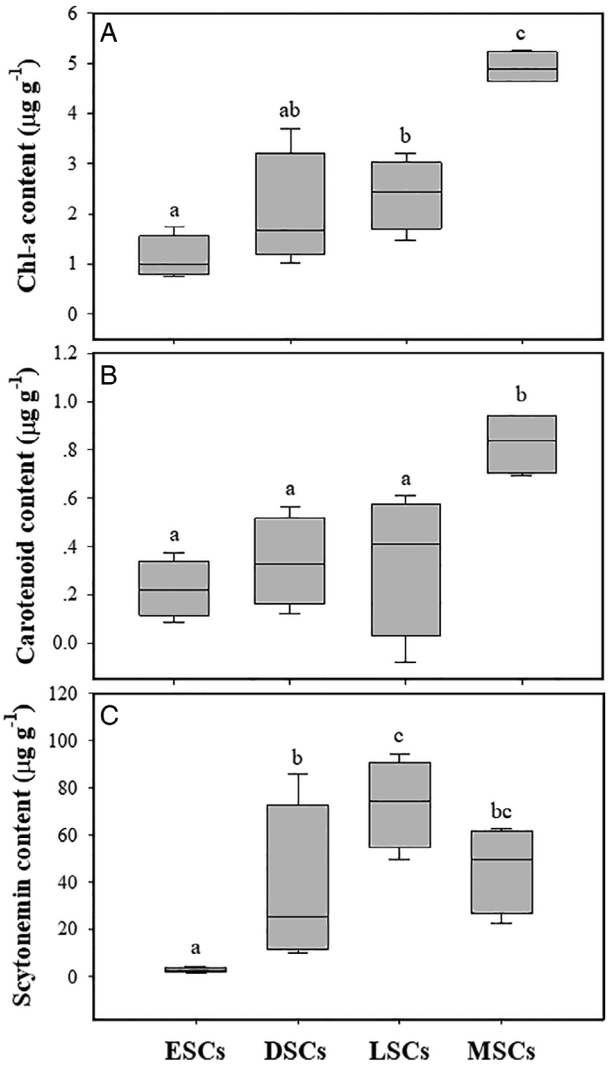

Fig. 5. Chlorophyll-a (Chl-a; A), carotenoids (B) and Scytonemin (C) contents in the different successional types of biocrusts. Boxes enclose the upper and lower inner quartiles with median values presented as solid lines and means of values as broken lines respectively. Whiskers indicate the extremes at the 5th and 95th percentile. For each parameter, the different lowercase letters indicate that the values are significantly different at the 0.05 level ($P < 0.05$).

Peninsula of Spain, although there are some differences in composition. Many cyanobacterial species in biocrusts are cosmopolitans, such as *M. vaginatus* and *M. steenstrupii* (Garcia-Pichel *et al*., 2013); however, there are some specifics that may be regional. For example, *Crinalium* was identified in the present study but was not found in previously mentioned studies.

Cyanobacteria in the biocrusts of the Gurbantunggut desert are mostly filamentous. In particular, filamentous non-nitrogen-fixing cyanobacterial species were the most abundant taxa, which are consistent with reports from many other drylands (e.g. Hagemann *et al*., 2014; Fernandes *et al*., 2018; Muñoz-Martín *et al*., 2019). This reflects the important role of filamentous cyanobacteria in the formation and maintenance of biocrusts, especially the bundle-forming filamentous cyanobacteria, such as the species of the genus *Microcoleus*. The filaments entangle soil particles, and secrete polysaccharides, cementing soil grains to form a fine crust structure (Lan *et al*., 2014; Mugnai *et al*., 2018). The most common heterocystous nitrogen-fixing filamentous cyanobacteria in our study were in the genera of *Nostoc*, *Scytonema* and *Tolypothrix*, although some other low abundance of nitrogen-fixing genera, such as *Calothrix*, were also found with Cydrasil analysis (Fig. S1), while this genus is typical of North American biocrusts (Yeager *et al*., 2007).

In addition to the filamentous cyanobacteria, there are abundant unicellular colonial cyanobacteria in the Gurbantunggut desert biocrusts. Most are in the genus *Chroococcidiopsis*, which is the major unicellular biocrust cyanobacterial genus (Hagemann *et al*., 2014; Williams *et al*., 2016; Muñoz-Martín *et al*., 2019). However, compared with other biocrust cyanobacterial communities (Steven *et al*., 2012; Dojani *et al*., 2014; Fernandes *et al*., 2018), the relative abundance of *Chroococcidiopsis* in the Gurbantunggut biocrusts is higher, sometimes exceeding 30% of total cyanobacterial abundance (Fig. 3), which may likely do with the extreme arid environment of this setting (Billi *et al*., 2000). Globally, *Chroococcidiopsis* variants have been regarded as common primary producers occurring in either hot or cold extreme arid deserts (Bahl *et al*., 2011).

The most dominant OTU across all biocrusts was *M. vaginatus* in the Gurbantunggut desert. This species has also been found to be dominant in other soil biocrusts worldwide (e.g. Starkenburg *et al*., 2011; Couradeau *et al*., 2019), and has been considered the most abundant soil cyanobacterium globally (Garcia-Pichel, 2003). The mean relative abundance of *M. vaginatus* in the present study was 43% of all cyanobacterial reads, which is likely to be caused by the low sensitivity of *M. vaginatus* to aridity than other biocrust cyanobacteria, such as the nitrogen-fixing cyanobacteria *Scytonema* and filamentous non-nitrogen-fixing cyanobacteria *M. steenstrupii* (Fernandes *et al*., 2018). Therefore, with the decline of precipitation in some areas under the global climate change, our results suggest that biocrust cyanobacteria community may develop towards the community structures with more abundance of *M. vaginatus* and *Chroococcidiopsis* spp.

Cyanobacterial community shift associated with biocrust succession

Our results reveal a clear cyanobacterial community shift associated with biocrust succession. ESCs and DSCs were mainly dominated by *M. vaginatus*, while

nitrogen-fixing and unicellular colonial cyanobacteria, such as *Chroococcidiopsis* spp. and *Nostoc* spp., occurred profusely in LSCs and MSCs (Fig. 3A). The relative abundance of different species in the genus *Microcoleus* also changed with biocrust succession (Fig. S1A). Garcia-Pichel *et al*. (2013) first observed biocrust cyanobacterial substitution between different species in the genus *Microcoleus* and deduced this was largely driven by temperature. They proposed that *M*. *vaginatus* was more psychrotolerant, and *M*. *steenstupii* was thermotolerant; therefore, climatic warming could lead to the replacement of *M*. *vaginatus* to *M*. *steenstrupii* in many dryland biocrusts. To some extent, our data also support this hypothesis. With biocrust succession, large quantities of scytonemin and carotenoids pigments develop (Fig. 5), giving later successional biocrusts, such as LSCs and MSCs, the ability to absorb more solar radiation energy, reducing biocrust albedo, thereby increasing biocrust temperature (Redfield *et al*., 2002; Couradeau *et al*., 2016). The resulting elevated temperatures may be unfavourable for the growth of *M*. *vaginatus*, which is further supported by the decreased relative abundance of *M*. *vaginatus* in LSCs and MSCs (Fig. 3A). Overall, the results of our study are in agreement with current models of biocrust cyanobacterial community shift derived from North American biocrusts (Garcia-Pichel and Wojciechowski, 2009; Garcia-Pichel *et al*., 2013), but we could define important novel aspects for some forms that are not the main, dominant types, and we could clearly demonstrate that biocrust succession actually involves significant increases with development in nitrogen-fixing cyanobacterial relative abundance, even as cyanobacterial populations become less dominant as lichens and mosses appear.

Functionally, community shift associated with increasing photosynthetic biomass (Chl-a content) suggests that the carbon-fixing role of cyanobacteria was gradually replaced with more cyanobacteria contributing to nitrogen fixation as biocrust succession progresses. This community shift may also relate to the differences in biocrust water absorption/retention between succession types, as well the sensitivity of biocrust cyanobacteria to moisture conditions. Nitrogen-fixing cyanobacteria *Scytonema* spp. has been regarded as the most sensitive biocrust taxa to drought (compared with *M*. *vaginatus* and *M*. *steenstrupii*; Fernandes *et al*., 2018), and biocrust water absorption/retention ability increases with their ecological succession (Redfield *et al*., 2002; Lan *et al*., 2015). As a result, a large proportion of nitrogen-fixing cyanobacteria are found in the later successional biocrusts (Housman *et al*., 2006; Couradeau *et al*., 2016). However, with decreasing moisture availability in the future (Huang *et al*., 2016), cyanobacterial community substitution associated with biocrust succession thus may be slowed down or even prevented.

A combination of climate change and increased soil disturbance is predicted to reduce biocrust coverage (Rodriguez-Caballero *et al*., 2018) and favour succession back to cyanobacterial soil crusts in some areas (Housman *et al*., 2006). This reversal of biocrust succession may result in a community shift to *M*. *vaginatus* dominated biocrust communities. At the same time, increasing aridity may cause the replacement of the nitrogen-fixing cyanobacteria (such as *Scytonema* spp.) by non-nitrogen-fixing and drought-tolerant filamentous cyanobacteria, such as *M*. *vaginatus* (e.g. Fernandes *et al*., 2018). However, there is some uncertainty because *M*. *vaginatus* is very sensitive to warming (Garcia-Pichel *et al*., 2013; Couradeau *et al*., 2016). In addition, nitrogen-fixing *Scytonema* also prefer warmer biocrust habitats (Muñoz-Martín *et al*., 2019). Therefore, with increasing aridity, warming and disturbance occurring in conjunction, it is still difficult to draw a unified conclusion on how the biocrust cyanobacterial community will develop and change in the future, but it will depend on the relative strengths of each factor. In a given region, several factors may work together to form a specific biocrust distribution and community compositions. Nevertheless, the sensitivity of biocrust cyanobacteria to aridity, warming and disturbances makes them potentially very good indicators of environmental change.

Effects of cyanobacteria on biocrust carbon and nitrogen storage

Biocrusts are widely distributed in dryland regions and are estimated to account for approximately 12% of the global land area (Rodriguez-Caballero *et al*., 2018); therefore, they are of great significance in carbon and nitrogen contribution in drylands and global biogeochemical cycle (Elbert *et al*., 2012). Our results regarding biocrust total carbon and total nitrogen contents increased with biocrust succession (Fig. 4C), are in agreement with the results of Garcia-Pichel and Belnap (1996), and those of Couradeau *et al*. (2016). The higher total carbon in the LSCs and MSCs could be explained by the increase of photosynthetic biomass (Fig. 5A) and carbon fixation ability (Lan *et al*., 2017) in the later successional types; while the higher total nitrogen in the later successional biocrusts was accompanied by the increasing relative abundance of nitrogen-fixing cyanobacteria (Fig. 4B), such as *Nostoc* and *Scytonema*.

The previous work in the Tengger Desert found that cyanobacterial and microalgal biomass decreased along with biocrust development and succession (Wu *et al*., 2014). Together, these previous and present results indicate that the contribution of cyanobacteria to biocrust carbon is gradually reduced with succession. An increasing number of lichens and mosses occupy a greater number

of biocrust niches, competing for light and water resources, and leaving the cyanobacteria with diminishing living space and resources. Although cyanobacterial relative abundance decreased significantly along with the succession, our nifH gene data revealed cyanobacteria always represented the vast majority of biocrust nitrogen-fixing organisms (approximately 92% of the nifH genes on average), and this is in agreement with the results from North American biocrusts (Yeager *et al*., 2007). In addition, non-cyanobacterial nitrogen fixers, however, may be also important in biocrust nitrogen fixation, particularly during the earliest phases of biocrust succession (Pepe-Ranney *et al*., 2016), in mutualistic association with *M*. *vaginatus* (Couradeau *et al*., 2019; Nelson *et al*., 2021).

Our results suggest the cyanobacterial community structure shift reflects the metabolism characteristics of the different successional biocrusts. This is in turn also closely related to biocrust ecological functions, such as carbon and nitrogen fixation and storage. With increasing aridity, warming and disturbance, biocrust cyanobacterial community structure associated with ecological succession could also be affected. Any reverse of biocrusts to early successional stages, such as cyanobacterial soil crusts, not only means dominant photosynthetic organisms such as lichens and mosses in the biocrusts being replaced by cyanobacteria but also the relative abundance of nitrogen-fixing cyanobacteria will be at risk of decline, which eventually leads to a decline in carbon and nitrogen storages in the dryland biocrusts.

Conclusion

This study of 16S rRNA and nifH genes in different successional biocrusts from the Gurbantunggut desert in China shows that cyanobacterial community shift accompanies biocrust succession, with cyanobacterial relative abundance becoming lower as the succession processes. However, heterocystous *Nostoc*, *Scytonema* and *Tolypothrix* always represent the majority of biocrust nitrogen-fixing organisms, contributing an average of 92% of the nifH genes. The specific cyanobacterial community in the extreme arid Gurbantunggut desert is mainly characterized by filamentous *M*. *vaginatus* with abundant unicellular colonial *Chroococcidiopsis* spp., suggesting that with the likely decline of water availability, biocrust cyanobacteria communities may develop community structures with greater abundances of *M*. *vaginatus* and *Chroococcidiopsis* spp. Moreover, cyanobacterial community analysis demonstrates that filamentous non-nitrogen-fixing cyanobacterial communities are gradually replaced by nitrogen-fixing and unicellular colonial communities along with the biocrust succession. Combined with biocrust carbon and nitrogen analysis, our results suggest the carbon-fixing role of biocrust cyanobacteria is gradually replaced with more cyanobacteria contributing to nitrogen fixation as succession progresses. The cyanobacteria present in each of the successional biocrusts have different sensitivities to moisture, temperature and disturbances, which makes them potentially very good indicators of environmental change, and require us to consider biocrusts types when analysing cyanobacterial community structure. These results also suggest any activity that reverses or resets biocrust succession will influence the cyanobacterial community structure, affecting ecological functions, such as carbon and nitrogen fixation and store in drylands.

Experimental procedures

Experimental region

The study sites are located in the Fukang region of Xinjiang Uygur Autonomous Region, located on the southern edge of the Gurbantunggut Desert (44°29′-44°44′N, 88°19′-88°39′E). It has a temperate continental climate and an altitude of 520–550 m above sea level. The annual average air temperature is 7.3°C with the extreme minimum temperature lower than −30°C, and the average annual precipitation is approximately 79.5 mm, falling mainly from April to July, while the annual potential evaporation is more than 2600 mm (Zhang *et al*., 2007; Zhou *et al*., 2020). The region is covered by extensive fixed and semi-fixed sand dunes. Soils are sandy, composed of 73%–83% sand, which support a sparse natural vegetation cover dominated by *Haloxylon ammodendron* and *H*. *persicum* (Zhang *et al*., 2007; Zhou *et al*., 2012, 2020). In between vegetation patches, most of the surface is covered by biocrusts, including cyanobacterial, lichen and moss soil crusts (Zhang *et al*., 2007; Li *et al*., 2016).

Sample collection

Biocrusts were collected from two sites. Site 1 (44°44′ N; 88°39′E) was characterized by a low cover (*c*. 10%) and light grey of ESCs. In contrast, biocrust cover at site 2 (44°29′ N; 88°19′E) exceeded 50% of the soil surface in places, and there was a broader range of well-developed biocrust types, with dark grey DSCs, black LSCs and brown MSCs. In this study, the above mentioned four biocrust types were collected to represent the different stages of ecological succession (Table 1). Each biocrust type was randomly collected at four different locations away from shrubs (at least 0.5 m), and all the sampling locations were separated from each other over 20 m. Biocrust samples were carefully scooped from the soil surface with a small trowel to ensure the natural

thickness of biocrusts was collected. One set of samples were placed in small tubes and stored in a −80°C fridge for subsequent DNA extraction; the other set was directly placed in Petri dishes and kept in a desiccator for subsequent physicochemical analysis.

Biocrust development index calculation

Major biocrust photosynthetic types were observed and identified with a binocular microscope/stereomicroscope according to the reference guides of Hu *et al*. (1980) and Rosentreter *et al*. (2007). Biocrust thickness (TH) was determined using a Vernier calliper, and an index of biocrust development (DI) was calculated as follows:

$$DI_i = TH_i \times Chl_i / (TH_{max} \times Chl_{max}) \quad (1)$$

where DI_i indicates the biocrust development index in a given sample *i*. TH_i and Chl_i are biocrust thickness and Chl-a content (analysing details are in the next section) in the sample *i*; while TH_{max} and Chl_{max} are respectively the maximum biocrust thickness and Chl-a content across all the samples.

Pigment, total carbon and nitrogen analysis

For biocrust pigment, total carbon and total nitrogen analysis, samples were first ground with mortar and pestle and then passed through a 50-mesh sieve (300 μm). The pigment extraction was carried out in darkness over 12 h using 100% acetone at 4°C. The extract solutions were centrifuged at 8000 rpm for 10 min, and the absorption values at 384, 490 and 663 nm of the supernatant solution were determined using an UV-spectrophotometer (Beijing Persee General Instruments, China). The contents of Chl-a, carotenoids and scytonemin were calculated according to the trichromatic equations of Garcia-Pichel and Castenholz (1991). To determine the total nitrogen content of the biocrusts, the ground samples were digested at 121°C for 30 min with alkaline potassium persulfate, and spectrophotometry was used to determine the concentrations using methods described by He *et al*. (2019). Total carbon content for the ground biocrust samples was measured using a Vario TOC analyser without any acid treatment (Elementar, Germany).

DNA extraction and PCR amplification

DNA extraction for each biocrust sample was carried out according to the instructions of the manufacturer of the soil DNA extraction kit (Omega, USA). DNA concentration and purity were determined by a NanoDrop2000 spectrophotometer (Thermo Scientific, USA), and DNA extraction quality was detected using 1% agarose gel electrophoresis. Thereafter, the 16S rRNA gene was amplificated with primers 338F (5′-ACTCCTACGGGAGGCAGCAG-3′) and 806R (5′-GGACTACHVGGGTWTCTAAT-3′; Couradeau *et al*., 2016); while nifH gene was amplified with primers nifH-F (5′-AAAGGYGGWATCGGYAARTCCACCAC-3′) and nifH-R (5′-TTGTTSGCSGCRTACATSGCCATCAT-3′; Fiorentino *et al*., 2017). Both of the amplification systems (20 μl) contained 4 μl of 5× FastPfu buffer, 2 μl of 2.5 mM dNTPs, 0.8 μl of each primer (5 μM each), 0.4 μl of FastPfu polymerase, 0.2 μl of bovine serum albumin and 10 ng of the template DNA. The PCR amplification procedures were as follows: initial denaturation at 95°C for 3 min, followed by 27/35 cycles (27 cycles for 16S rRNA gene and 35 cycles for nifH gene) of denaturation at 95°C for 30 s, annealing at 55°C for 30 s, and extension at 72°C for 45 s, and a final extension at 72°C for 10 min. All the PCR amplifications were carried out using a GeneAmp 9700 PCR System (ABI, USA).

High-throughput sequencing

The 16S rRNA and nifH gene amplification products were extracted using 2% agarose gel and purified by the AxyPrep DNA Gel Extraction Kit (Axygen Biosciences, USA). All the purified gene products were quantified using a QuantiFluor™-ST quantitative system (Promega, USA) and then sequenced on the Miseq PE300 according to the Illumina MiSeq platform standard protocols (Illumina, USA). Sequencing was performed by the Major BioTech (Shanghai, China). All the sequence data were deposited to NCBI Short Read Archive database under BioProjects PRJNA723170 and PRJNA723272.

16S rRNA/nifH gene sequence analysis

All the 16S rRNA/nifH gene raw sequences were demultiplexed and quality-controlled using Trimmomatic trimmer and merged using Fast Length Adjustment of SHort reads (FLASH). The chimeric sequences were identified and removed using the UCHIME, and then each sample obtained 23 912–32 432 16S rRNA gene sequences and 27 054–54 404 nifH gene sequences (Table 1). The effective sequences were clustered into different OTUs with a 97% similarity cut-off using UPARSE (version 7.1 http://drive5.com/uparse/), and the representative sequence of each OTU was given. The RDP classifier algorithm (http://rdp.cme.msu.edu/) was then used to identify the OTUs against the Silva/FunGene database (http://www.arb-silva.de/ and http://fungene.cme.msu.edu/; Silva database for 16S rRNA gene and FunGene database for nifH gene) with the confidence threshold of 70%. The Good's coverage ranged from 99.24% to 99.98%, indicating that most of the

biocrust microorganisms containing the 16s rRNA/nifH gene had been revealed (Table 1).

Cyanobacterial sequence analysis

Regardless of the 16S rRNA or nifH genes, the non-cyanobacterial and chloroplast sequences were eliminated from our dataset, and all of the OTU representative sequences annotated as cyanobacteria were manually blasted against the GenBank database to match with the cultivated cyanobacterial sequences. Those sequences with more than 97% similarity and derived from specific cyanobacteria-research articles/labs were retrieved. The cyanobacterial OTU representative sequences were then aligned along with the sequences retrieved from the GenBank database to ultimately determine the phylogenic (taxonomic) position of each OTU (see Statistical analysis for the details). In addition, the DADA2 (Callahan *et al*., 2016) and Cydrasil (Roush *et al*., 2021) were also used to check our cyanobacterial taxa (see Supplementary Material for the details). Cyanobacterial relative abundance in this study was defined as the percentage of cyanobacterial 16S rRNA gene sequences in all 16S rRNA gene sequences, and the relative abundance of nitrogen-fixing cyanobacteria in nitrogen-fixing microorganisms was defined as the percentage of cyanobacterial nifH gene sequences in all nifH gene sequences. To further analyse the cyanobacterial community structure, the relative abundance of each cyanobacterial taxon (such as clade, genus) was defined as the percentage of the corresponding 16S rRNA gene sequences in cyanobacterial 16S rRNA gene sequences.

Statistical analysis

The variation of each parameter was analysed by one-way ANOVA or non-parametric test according to their normality, and the variation analysis was performed on Statistical Product and Service Solutions (SPSS v.20). Bacterial communities at phylum level were clustered by Hierarchical Clustering using a Multi Experiment Viewer. The phylogenies of 16S rRNA and nifH gene sequences (including the OTU representative sequences and the retrieved sequences from GenBank) were analysed using Maximum Likelihood Tree with 1000 bootstrap replications, and the gaps/missing data were completely deleted. The Maximum Likelihood Tree was performed on a Mega 6.0 software. Adjusted R^2 values were evaluated by Curve Estimation to fit curves using Sigmaplot 12.5 software.

Acknowledgements

This study was kindly supported by the National Natural Science Foundation of China (Nos. U2003120, U1703120 and 31670456), by the Strategic Priority Research Program of the Chinese Academy of Sciences (No. XDA17010502) and by the Youth Innovation Promotion Association CAS (No. 2017385).

References

Bahl, J., Lau, M.C.Y., Smith, G.J.D., *et al*. (2011) Ancient origins determine global biogeography of hot and cold desert cyanobacteria. *Nat Commun* **2**: 163.

Belnap, J. (2006) The potential roles of biological soil crusts in dryland hydrological cycles. *Hydrol Process* **20**: 3159–3178.

Billi, D., Friedmann, I.E., Hofer, K.G., Grilli-Caiola, M., and Ocampo-Friedmann, R. (2000) Ionizing-radiation resistance in the desiccation-tolerant cyanobacterium Chroococcidiopsis. *Appl Environ Microbiol* **66**: 1489–1492.

Büdel, B., Colesie, C., Green, T.G., Grube, M., Lázaro Suau, R., Loewen-Schneider, K., *et al*. (2014) Improved appreciation of the functioning and importance of biological soil crusts in Europe: the Soil Crust International Project (SCIN). *Biodivers Conserv* **23**: 1639–1658.

Callahan, B.J., McMurdie, P.J., Rosen, M.J., Han, A.W., Johnson, A.J.A., and Holmes, S.P. (2016) DADA2: high-resolution sample inference from Illumina amplicon data. *Nat Methods* **13**: 581–583.

Couradeau, E., Giraldo-Silva, A., Martini, F.D., and Garcia-Pichel, F. (2019) Spatial segregation of the biological soil crust microbiome around its foundational cyanobacterium, Microcoleus vaginatus, and the formation of a nitrogen-fixing cyanosphere. *Microbiome* **7**: 55.

Couradeau, E., Karaoz, U., Lim, H.C., da Rocha, U.N., Northen, T., Brodie, E., and Garcia-Pichel, F. (2016) Bacteria increase arid-land soil surface temperature through the production of sunscreens. *Nat Commun* **7**: 10373.

Dojani, S., Kauff, F., Weber, B., and Büdel, B. (2014) Genotypic and phenotypic diversity of cyanobacteria in biological soil crusts of the succulent Karoo and Nama Karoo of southern Africa. *Microb Ecol* **67**: 286–301.

Elbert, W., Weber, B., Burrows, S., Steinkamp, J., Büdel, B., Andreae, M., *et al*. (2012) Contribution of cryptogamic covers to the global cycles of carbon and nitrogen. *Nat Geosci* **5**: 459–462.

Eldridge, D.J., and Delgado-Baquerizo, M. (2019) The influence of climatic legacies on the distribution of dryland biocrust communities. *Glob Chang Biol* **25**: 327–336.

Eldridge, D.J., and Leys, J.F. (2003) Exploring some relationships between biological soil crusts, soil aggregation and wind erosion. *Journal of Arid Environments*, **53**: 457–466. https://doi.org/10.1006/jare.2002.1068

Elliott, D.R., Thomas, A.D., Hoon, S.R., and Sen, R. (2014) Niche partitioning of bacterial communities in biological crusts and soils under grasses, shrubs and trees in the Kalahari. *Biodivers Conserv* **23**: 1709–1733.

Felde, V.J.M.N.L., Peth, S., Uteau-Puschmann, D., Drahorad, S., and Felix-Henningsen, P. (2014) Soil

microstructure as an under-explored feature of biological soil crust hydrological properties: case study from the NW Negev Desert. *Biodivers Conserv*, **23**: 1687–1708. https://doi.org/10.1007/s10531-014-0693-7

Fernandes, V., de Lima, M., Maria, N., Roush, D., Rudgers, J., Collins, S.L., and Garcia-Pichel, F. (2018) Exposure to predicted precipitation patterns decreases population size and alters community structure of cyanobacteria in biological soil crusts from the Chihuahuan Desert. *Environ Microbiol* **20**: 259–269.

Fiorentino, N., Ventorino, V., Rocco, C., Cenvinzo, V., Agrelli, D., Gioia, L., *et al*. (2017) Giant reed growth and effects on soil biological fertility in assisted phytoremediation of an industrial polluted soil. *Sci Total Environ* **575**: 1375–1383.

Garcia-Pichel, F. (2003) Desert environments: biological soil crusts. In *Encyclopedia of Environmental Microbiology*. New York: John Wiley, pp. 1019–1023.

Garcia-Pichel, F., and Belnap, J. (1996) The microenvironments and microscale productivity of cyanobacterial desert crusts. *J Phycol* **32**: 774–782.

Garcia-Pichel, F., and Belnap, J. (2001) Small-scale environments and distribution of biological soil crusts. In *Biological Soil Crusts: Structure, Function, and Management*. Berlin: Springer, pp. 193–201.

Garcia-Pichel, F., and Castenholz, R.W. (1991) Characterization and biological implications of scytonemin, a cyanobacterial sheath pigment. *J Phycol* **27**: 395–409.

Garcia-Pichel, F., Loza, V., Marusenko, Y., Mateo, P., and Potrafka, R.M. (2013) Temperature drives the continental-scale distribution of key microbes in topsoil communities. *Science* **340**: 1574–1577.

Garcia-Pichel, F., and Pringault, O. (2001) Cyanobacteria track water in desert soils. *Nature* **413**: 380–381.

Garcia-Pichel, F., and Wojciechowski, M.F. (2009) The evolution of a capacity to build supra-cellular ropes enabled filamentous cyanobacteria to colonize highly erodible substrates. *PLoS One* **4**: e7801.

Hagemann, M., Henneberg, M., Felde, V.J.M.N.L., Drahorad, S.L., Berkowicz, S.M., Felix-Henningsen, P., and Kaplan, A. (2014) Cyanobacterial diversity in biological soil crusts along a precipitation gradient, Northwest Negev Desert, Israel. *Microb Ecol* **70**: 219–230.

He, X., Sun, Q., Xu, T., Dai, M., and Wei, D. (2019) Removal of nitrogen by heterotrophic nitrification–aerobic denitrification of a novel halotolerant bacterium *Pseudomonas mendocina* TJPU04. *Bioprocess Biosyst Eng* **42**: 853–866.

Housman, D.C., Powers, H.H., Collins, A.D., and Belnap, J. (2006) Carbon and nitrogen fixation differ between successional stages of biological soil crusts in the Colorado plateau and Chihuahuan Desert. *J Arid Environ* **66**: 620–634.

Hu, H., Li, R., Wei, Y., Zhu, H., Chen, J., and Shi, Z. (1980) *Freshwater Algae in China*. Shanghai: Shanghai Science and Technology Press (in Chinese).

Lan, S., Ouyang, H., Wu, L., Zhang, D., and Hu, C. (2017) Biological soil crust community types differ in photosynthetic pigment composition, fluorescence and carbon fixation in Shapotou region of China. *Appl Soil Ecol* **111**: 9–16.

Lan, S., Thomas, A.D., Tooth, S., Wu, L., and Hu, C. (2019) Small-scale spatial heterogeneity of photosynthetic fluorescence associated with biological soil crust succession in the Tengger Desert, China. *Microb Ecol* **78**: 936–948.

Lan, S., Wu, L., Zhang, D., and Hu, C. (2015) Analysis of environmental factors determining development and succession in biological soil crusts. *Sci Total Environ* **538**: 492–499.

Lan, S., Zhang, Q., Wu, L., Liu, Y., Zhang, D., and Hu, C. (2014) Artificially accelerating the reversal of desertification: cyanobacterial inoculation facilitates the succession of vegetation communities. *Environ Sci Technol* **48**: 307–315.

Li, H., Li, R., Rossi, F., Li, D., De Philippis, R., Hu, C., and Liu, Y. (2016) Differentiation of microbial activity and functional diversity between various biocrust elements in a heterogeneous crustal community. *Catena* **147**: 138–145.

Lin, L., Gettelman, A., Feng, S., and Fu, Q. (2015) Simulated climatology and evolution of aridity in the 21st century. *J Geophys Res-Atmos* **120**: 5795–5815.

Maier, S., Tamm, A., Wu, D., Caesar, J., Grube, M., and Weber, B. (2018) Photoautotrophic organisms control microbial abundance, diversity, and physiology in different types of biological soil crusts. *ISME J* **12**: 1032–1046.

Mugnai, G., Rossi, F., Felde, V.J., Colesie, C., Büdel, B., Peth, S., *et al*. (2018) Development of the polysaccharidic matrix in biocrusts induced by a cyanobacterium inoculated in sand microcosms. *Biol Fert Soils* **54**: 27–40.

Muñoz-Martín, M.Á., Becerra-Absalón, I., Perona, E., Fernández-Valbuena, L., Garcia-Pichel, F., and Mateo, P. (2019) Cyanobacterial biocrust diversity in Mediterranean ecosystems along a latitudinal and climatic gradient. *New Phytol* **221**: 123–141.

Nelson, C., Giraldo-Silva, A., and Garcia-Pichel, F. (2021) A symbiotic nutrient exchange within the cyanosphere microbiome of the biocrust cyanobacterium, *Microcoleus vaginatus*. *ISME J* **15**: 282–292.

Pepe-Ranney, C., Koechli, C., Potrafka, R., Andam, C., Eggleston, E., Garcia-Pichel, F., and Buckley, D.H. (2016) Non-cyanobacterial diazotrophs mediate dinitrogen fixation in biological soil crusts during early crust formation. *ISME J* **10**: 287–298.

Redfield, E., Barns, S.M., Belnap, J., Daane, L.L., and Kuske, C.R. (2002) Comparative diversity and composition of cyanobacteria in three predominant soil crusts of the Colorado plateau. *FEMS Microbiol Ecol* **40**: 55–63.

Reynolds, J.F., Smith, D.M.S., Lambin, E.F., Turner, .B.L., II, Mortimore, M., Batterbury, S.P.J., *et al*. (2007) Global desertification: building a science for dryland development. *Science* **316**: 847–851.

Rodriguez-Caballero, E., Belnap, J., Büdel, B., Crutzen, P.J., Andreae, M.O., Pöschl, U., *et al*. (2018) Dryland photoautotrophic soil surface communities endangered by global change. *Nat Geosci* **11**: 185–189.

Rodríguez-Caballero, E., Cantón, Y., Chamizo, S., Afana, A., and Solé-Benet, A. (2012) Effects of biological soil crusts on surface roughness and implications for runoff and erosion. *Geomorphology* **145-146**: 81–89.

Roncero-Ramos, B., Muñoz-Martín, M.A., Chamizo, S., Fernández-Valbuena, L., Mendoza, D., Perona, E., *et al*. (2019) Polyphasic evaluation of key cyanobacteria in biocrusts from the most arid region in Europe. *Peer J* **7**: e6169.

Rosentreter, R., Bowker, M., and Belnap, J. (2007) *A Field Guide to Biological Soil Crusts of Western U.S. Drylands*. Denver: U.S. Government Printing Office.

Roush, D., Giraldo-Silva, A., and Garcia-Pichel, F. (2021) Cydrasil 3, a curated 16S rRNA gene reference package and web app for cyanobacterial phylogenetic placement. *Scientific Data* **8.1**: 1–6.

Starkenburg, S.R., Reitenga, K.G., Freitas, T., Johnson, S., Chain, P.S.G., Garcia-Pichel, F., and Kuske, C.R. (2011) Genome of the cyanobacterium *Microcoleus vaginatus* FGP-2, a photosynthetic ecosystem engineer of arid land soil biocrusts worldwide. *J Bacteriol* **193**: 4569–4570.

Steven, B., Gallagos-Graves, L.V., Yeager, C.M., Belnap, J., Evans, J., and Kuske, C.R. (2012) Dryland biological soil crust Cyanobacteria show unexpected decreases in abundance under long-term elevated CO_2. *Environ Microbiol* **14**: 3247–3258.

Thomas, A.D. (2012) Impact of grazing intensity on seasonal variations in SOC and soil CO_2 efflux in two semiarid grasslands in southern Botswana. *Philos Trans R Soc B* **367**: 3076–3086.

Thomas, A.D., Elliott, D.R., Dougill, A.J., Stringer, L.C., Hoon, S.R., and Sen, R. (2018) The influence of trees, shrubs, and grasses on microclimate, soil carbon, nitrogen, and CO_2 efflux: potential implications of shrub encroachment for Kalahari rangelands. *Land Degand Dev* **29**: 1306–1316.

Williams, L., Loewen-Schneider, K., Maier, S., and Büdel, B. (2016) Cyanobacterial diversity of western European biological soil crusts along a latitudinal gradient. *FEMS Microbiol Ecol* **92**: fiw157.

Wu, L., Lan, S., Zhang, D., and Hu, C. (2013) Functional reactivation of photosystem II in lichen soil crusts after long-term desiccation. *Plant Soil* **369**: 177–186.

Wu, L., Zhang, G., Chen, X., Lan, S., Zhang, D., and Hu, C. (2014) Development and succession of biological soil crusts and the changes of microbial biomasses. *Environ Sci* **35**: 1479–1485.

Yeager, C.M., Kornosky, J.L., Morgan, R.E., Cain, E.C., Garcia-Pichel, F., Housman, D.C., *et al*. (2007) Three distinct clades of cultured heterocystous cyanobacteria constitute the dominant N_2-fixing members of biological soil crusts of the Colorado plateau, USA. *FEMS Microbiol Ecol* **60**: 85–97.

Zaady, E., Kuhn, U., Wilske, B., Sandoval-Soto, L., and Kesselmeier, J. (2000) Patterns of CO_2 exchange in biological soil crusts of successional age. *Soil Biol Biochem* **32**: 959–966.

Zhang, Y., Chen, J., Wang, L., Wang, X., and Gu, Z. (2007) The spatial distribution patterns of biological soil crusts in the Gurbantunggut Desert, northern Xinjiang, China. *J Arid Environ* **68**: 599–610.

Zhou, X., Tao, Y., Yin, B., Tucker, C., and Zhang, Y. (2020) Nitrogen pools in soil covered by biological soil crusts of different successional stages in a temperate desert in Central Asia. *Geoderma* **366**: 114166.

Zhou, X., Zhang, Y., and Downing, A. (2012) Non-linear response of microbial activity across a gradient of nitrogen addition to a soil from the Gurbantunggut Desert, northwestern China. *Soil Biol Biochem* **47**: 67–77.

Supporting Information

Additional Supporting Information may be found in the online version of this article at the publisher's web-site:

Appendix S1. Supporting Information.